Sulfide Precipitation During Hot Strip Mill of an if Steel

W. Regone[1]; A.M. Jorge Júnior[2] and O. Balancin[3]
[1] *pwir@iris.ufscar.br;* [2] *moreira@power.ufscar.br;* [3] *balancin@power.ufscar.br*
[1,2,3] *Department of Materials Engineering, UFSCar – Federal University of São Carlos*
Via Washington Luiz, Km 235 São Carlos - SP - Brazil, CEP: 13565-905

Abstract

Although precipitates in IF steels have been observed by many authors, they have yet to appear in stress vs. strain curves during laboratorial simulations. The flow behavior of an IF steel was investigated during multi-pass deformation under conditions similar to those of a hot strip mill by means of torsion tests. With short interpass times, there was a sharp and unexpected increase in the level of flow stress as the material was strained at temperatures of around 920°C, suggesting the presence of a hardening mechanism operating during the arrest time. TEM and X-ray chemical microanalysis techniques revealed the presence of precipitates such as TiS and $Ti_4C_2S_2$ (transformed *in situ* and finely precipitated) in samples quenched after straining.

Keywords: Hot Working, Interstitial Free Steel, Precipitation.

Introduction

The low level of interstitial elements and the annealing {111} texture confer characteristics of outstandingly deep drawability on interstitial free (IF) steels. During hot strip mill, the level of interstitial elements such as carbon and nitrogen, which are not removed by the steelmaking process, can be reduced by combining them with stabilizing elements. In titanium-stabilized steels, Ti combines with N prior to scavenging S and C. Because carbon is combined as a precipitate instead of forming an interstitial solid solution, IF steels are also non-aging, meeting the formability requirements for extra deep drawable steel grades [1].

In laboratorial simulations and in final shape products, the microstructure of this kind of steel has been found to consist of a highly ductile matrix of ferrite with imbedded precipitates such as TiC, TiS, $Ti_4C_2S_2$ and TiN [2-4]. Some authors have speculated that the traditional precipitation sequence, TiN, TiS, $Ti_4C_2S_2$ and TiC [2-4], occurs upon hot strip mill of titanium IF steels, during cooling from austenite to ferrite region, and that the precipitates are free-standing particles formed by nucleation and growth processes. Other article [5] have reported that the transformation of TiS into $Ti_4C_2S_2$ may be considered a hybrid of shear and diffusion, i.e., faulted Ti_8S_9 (9R) + 10[Ti] + 9[C] → $41/2Ti_4C_2S_2$ (or H, due to its hexagonal crystal structure). At low temperatures (≤930°C), the stabilization process continues through epitaxial growth of carbides in the H phase. This mechanism differs from the traditional view of stabilization, because the initially formed 9R sulfide particles undergo an *in situ* transformation into carbosulfides H by absorption of C and Ti.

The $Ti_4C_2S_2$ compound, reported to be the only ternary phase in the Ti-S-C system, has an $AlCCr_2$ type structure, space group $P6_3/mmc$, and lattice parameters a = 0.3210 and c = 1.120nm [6]. It has also been reported to occur as an inclusion of up to 20 μm in size in many other types of steels and alloys [7]. The crystal structure of TiS in ultra low carbon (ULC) steels has been described as 9R-$Ti_{1-x}S$ (R rhombohedral, nine-lattice layers in a unit cell), with (1-x)=Ti/S≈0.9, space group $R3m$, and lattice parameters a=0.34 and c=2.65 [8]. The M(C,N) phase in low carbon steels is commonly reported as Fm3m, with a=0.42 to 0.44 nm [9]. In

short, carbon can be stabilized in Ti-IF steels through the formation of carbosulfides (H) and/or carbides (MC_{1-x}).

Although these precipitates have been found in final products, their effect on the flow stress behavior in laboratorial simulations has not been identified. The main goal of this work was to investigate the influence of these precipitates on stress-strain curves under conditions similar to those of a hot strip mill.

Materials and Methods

The Ti stabilized IF steel used in this work was supplied by Companhia Siderúrgica Paulista (COSIPA-SP- Brazil) and its chemical composition is given in Table 1. Cylindrical specimens with 3.15 mm of effective radius and 20 mm of effective length were machined from hot rolled plates.

Table 1 – Chemical composition of the IF steel (wt%)

C	Mn	Si	Al	S	P	Ti	N
0.004	0.132	0.011	0.011	0.007	0.01	0.065	0.006

The mechanical tests were carried out on a computerized hot torsion machine described in detail in previous articles [10]. In order to prevent oxidation of the specimens, a quartz tube was coupled to the equipment, along the longitudinal axis of the furnace, through which argon balanced with 2% hydrogen was continuously flushed. This device also allowed for instantaneous injection of water to quench the specimens in order to retain the high-temperature microstructures for further observations. Stress-strain equivalent curves were calculated for each test based on torque and rotation angle measurements, using the Von Misses criteria [11].

To study the effect of precipitation on the stress-strain behavior under conditions similar to those of hot strip mill, samples of this material were subjected to multipass tests. In these experiments, the specimens were heated to 1200°C and held at this temperature for 10 min. They were then cooled down to 920°C and subjected to double straining tests [12] at a strain rate of 1 s^{-1} and interpass times ranging from 0.5 to 100 s, as schematically represented in Figure 1. In this kind of experiment, material softening or hardening after the first straining is analyzed. Based on Figure 2, the following equation was used to calculate softening after the first pass:

$$SF = \frac{(\sigma_D - \sigma_R)}{(\sigma_D - \sigma_Y)} \qquad (1)$$

where SF is the softening fraction.

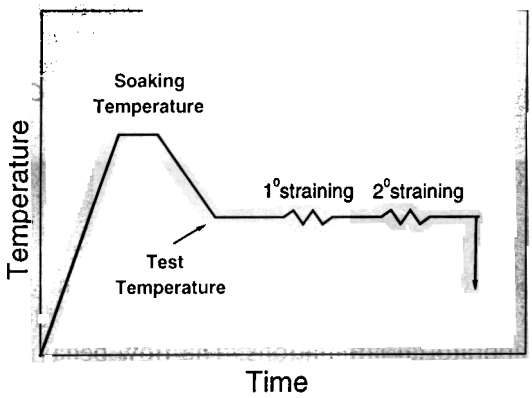

Figure 1: Schematic representation of thermal cycle employed in isothermal double straining tests

Both thin foils and carbon replicas were used for transmission electron microscopy (TEM) analyses. Several particles containing S and/or C in each sample were analyzed. A CM 120 TEM microscope equipped with an EDAX high angle detector (Z≥12) was used in this study. Parameters such as morphology, particle size and chemical composition were analyzed.

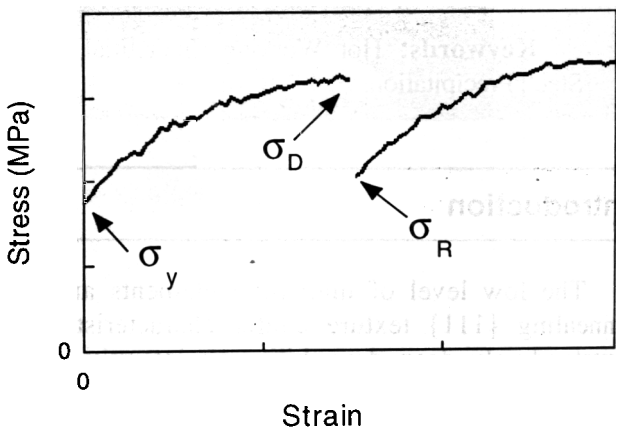

Figure 2: Reference stresses used in equation 1 to calculate the softening fraction

Results and Discussion

Figures 3a and b display the data from mechanical tests for the experiments carried out at 1000°C and 920°C, respectively. Figure 3a shows that, at 1000°C, this material softens in the arrest time, during all the imposed interpass times. On the other hand, Figure 3b shows a rising level of flow stress after short interpass times of 0,5 and 1s, indicating that the material hardens under these conditions. These different behaviors can be better seen in Figure 4, which plots the softening fraction determined by equation 1 as a function of the arrest time.

This diagram shows that, at 1000°C, the material softens under all the conditions investigated. Softening increases as the interpass time is increased, with the curve displaying a normal sigmoidal shape. The softening fractions determined at 920°C reveal that the material hardens in short-interval times, which is indicated by the negative values, suggesting the action of a hardening mechanism. This hypothesis is supported by experimental data comparing the curves obtained at 1000°C and 920°C. As can be seen, the curve that represents softening at 920°C can be divided into two different regions: the first with times of less than 5s and the second with times of more than 20s. This difference is caused by the hardening mechanism, which retards the softening processes in the shortest interpass times.

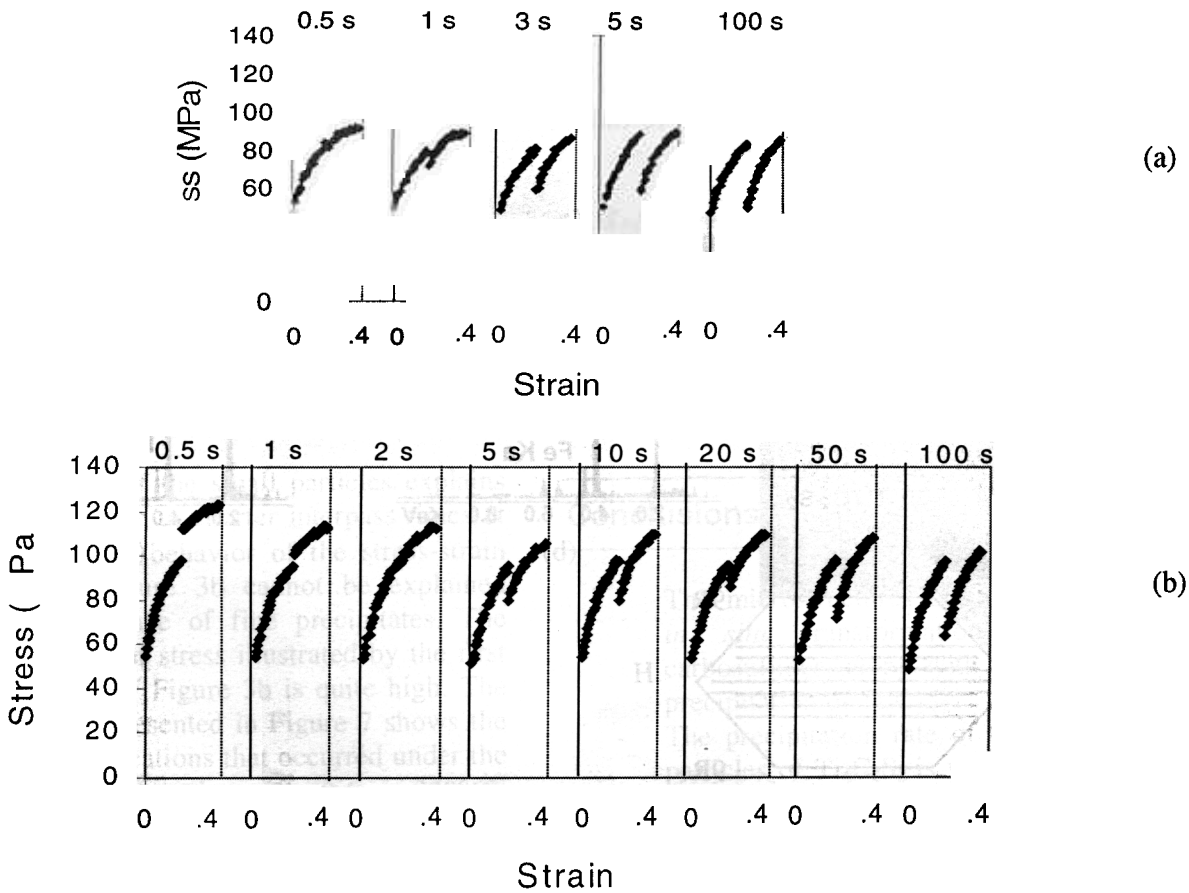

Figure 3: (a) stress vs. strain curves obtained from double hot torsion tests (1000°C, $1s^{-1}$), showing softening after interpass times ranging from 0.5 to 100 s. (b) stress vs. strain curves obtained from double hot torsion tests (920°C, $1s^{-1}$), showing hardening after interpass times of 0.5 and 1 s.

Microstructural observations of carbon extraction replicas after an arrest time of 0.5s at 920°C show a large number of particles, Figure 5a, some of which are sandwich-like, as indicated by arrows. The 9R-H-9R displays a sandwich-like morphology, with 9R on the outside and the H phase forming internal layers (Figure 5d). Figures 5b and c show the typical EDS spectrum of the H phase and the spectrum of the border of the particles of the 9R phase. TiS and isolated $Ti_4C_2S_2$ particles were observed along with the sandwich-like carbosulfides. This fact indicates the *in situ* transformation of TiS → $Ti_4C_2S_2$, as reported in the literature [5].

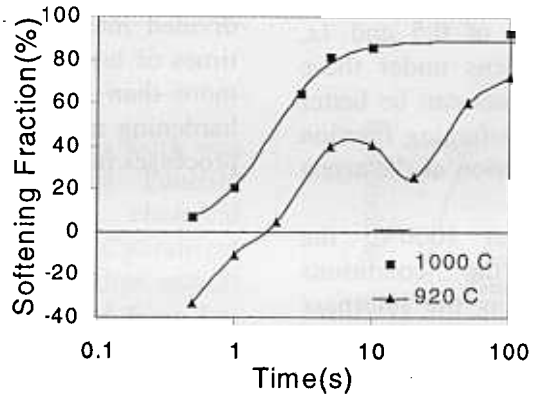

Figure 4: Softening curves obtained from tests shown in Figure 3, after application of equation 1. The negative values of the 920°C softening curve indicate the action of a hardening mechanism at lower arrest times.

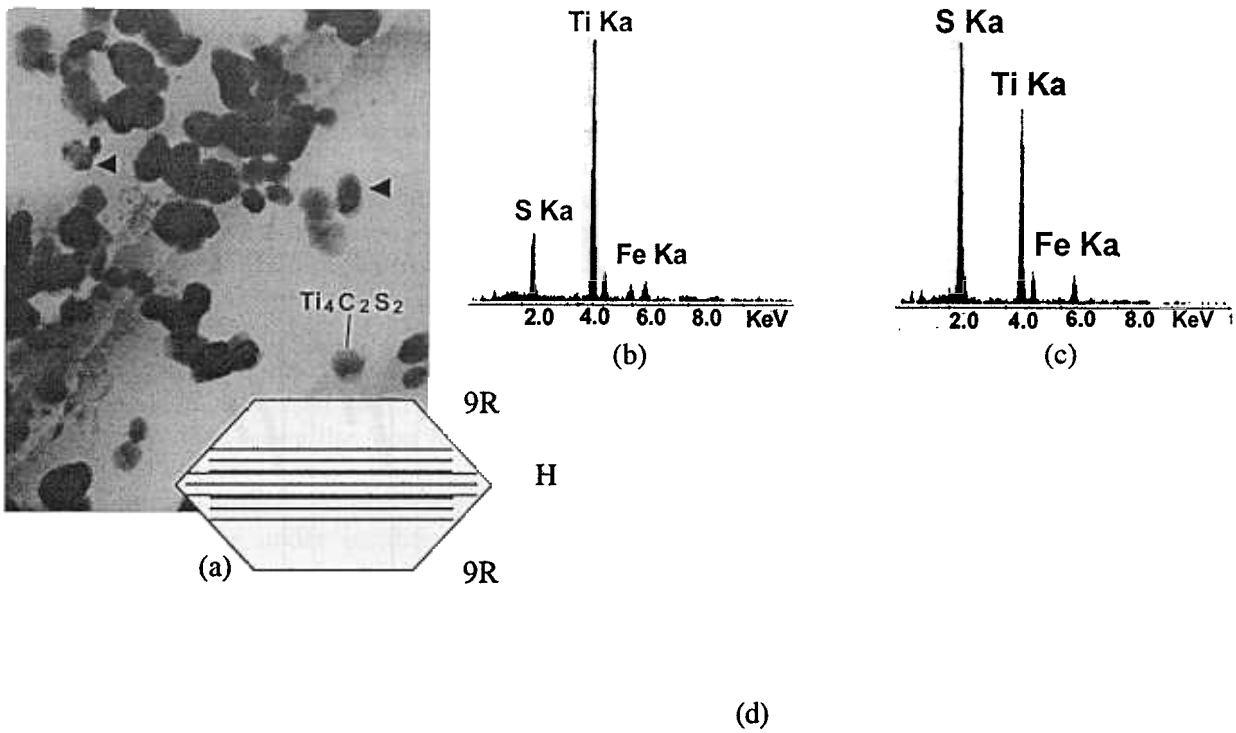

Figure 5: TEM micrograph showing multiphase, sandwich-like particles after 0.5s of interpass time at 920°C. (a) Carbon extraction replica. (b) Typical EDS spectrum from H phase ($Ti_4C_2S_2$). (c) Typical EDS spectrum of the border of the particles marked with arrows, showing the 9R phase (TiS). (d) Morphology of 9R-H-9R sandwich-like particles formed during 9R→H *in situ* transformation.

Although precipitates were observed after 0,5 s, their size suggested that they could not have acted on the softening process [13]. The medium size of these particles was around 400nm. Thin foil TEM analyses were performed to investigate the presence of small particles in this sample. Figure 6a shows particles with smaller sizes than those observed in Figure 5a, i.e., around 10 nm. This photomicrography was obtained from a $Ti_4C_2S_2$ (103) spot, ensuring that the precipitates shown were of $Ti_4C_2S_2$. The EDS spectrum shown in Figure 6b, a typical one for this phase, confirms this statement.

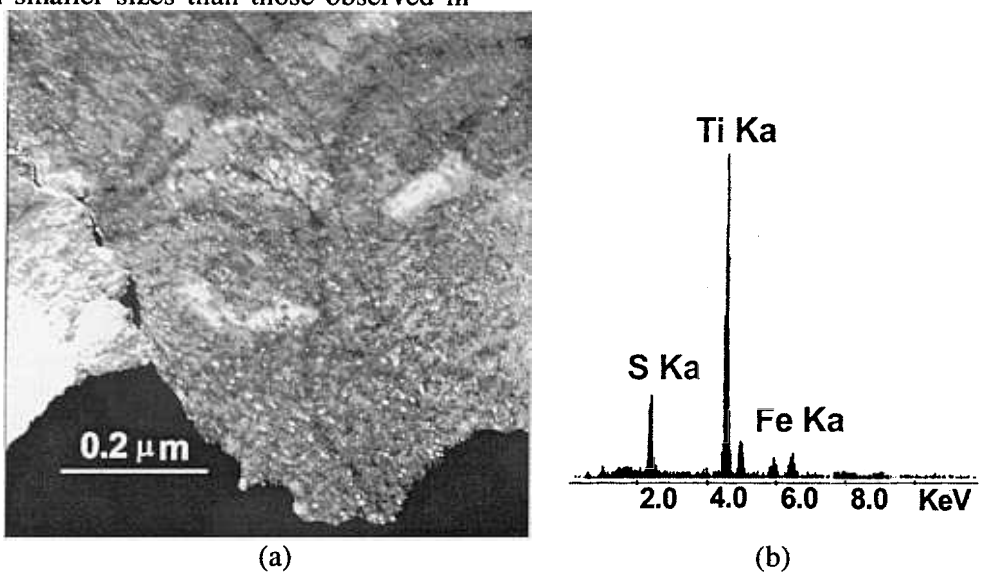

Figure 6: (a) Dark field obtained from a $Ti_4C_2S_2$ (103) spot, showing that the particle size is smaller than that in Figure 5a. (b) Typical EDS spectrum for $Ti_4C_2S_2$ obtained from these particles.

An observation of the small particles explains the low softening rate in shorter interpass times at 920°C; however, the behavior of the stress-strain curve shown in Figure 3b cannot be explained solely by the presence of fine precipitates. The change of the level of stress illustrated by the first and second curves of Figure 3b is quite high. The photomicrography presented in Figure 7 shows the high density of dislocations that occurred under the conditions described in Figure 3b (0,5s at 920°C). Based on this image and taking into account the precipitates obtained, one can infer that precipitation begins at close to 0,5s and delays static recovery, enhancing the material's strength during the arrest time. After 20s, the precipitates coarsen, ceasing to act on the softening process.

Conclusions

The microstructures observed confirm the *in situ* transformation of 9R into carbosulfides, along with the free-standing precipitation of $Ti_4C_2S_2$.

The precipitation rate of the free-standing particles of $Ti_4C_2S_2$ is very fast and occurs before the materials soften. These precipitates can harden Ti-IF steel at the arrest time under hot strip mill conditions.

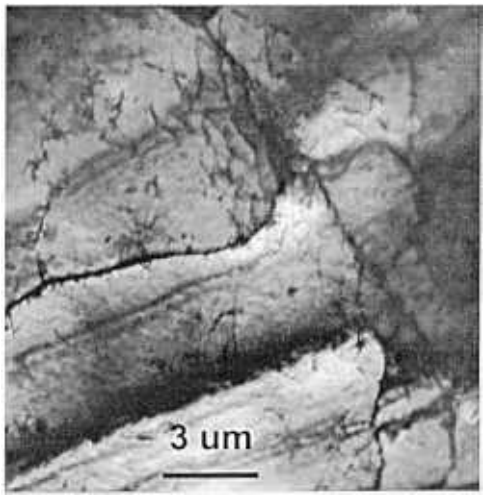

Figure 7: Photomicrography showing the high density of dislocations observed after an interpass time of 0,5s at 920°C.

Acknowledgments

The authors thank the Brazilian research funding institutions FAPESP and CNPq for their financial support of this work.

References

[1] Hoile, S., Mat. Sci. Tech, 2000, vol. 16, pp.1079-1093.
[2] Mendoza, R.; Huante, J.; Alanis, M.; Gonzáles-Rivera, C. and Juzarez-Islas, J.A., Mat. Sci. Eng. A, 2000, vol 276, pp. 203-209.
[3] Hua, M.; Garcia, C.I. and DeArdo, A.J., Scr. Metall. Mater., 1993, vol. 28, pp. 973-978.
[4] Yoshinaga, M.; Ushioda, K.; Akamatsu, S. and Akisue, O., ISIJ Int., 1994, vol. 34, pp. 24-32.
[5] Hua, M.; Garcia, C.I. and DeArdo, A.J., Metall. Mat. Trans. A, 1997, vol. 28A, pp. 1769-1780.
[6] Kudielka, V.H. and Rodhe, H., Kristallogr., Kristallgeom., Kristallph., Kristallchem., 1960, vol. 114, pp. 447-456.
[7] Maloney, J.L. and Garrison, W.M., Scr. Metall., 1989, vol. 23, pp. 2097-2100.
[8] Prikryl, M.Y.; Lin, P. and Subramanian, S.V., Scr. Metall. Mater., 1990, vol. 24, pp. 357-380.
[9] Gladmann
[10] Jorge Jr, A.M. e BALANCIN, 0.: R.E.M. – Revista da Escola de Minas, 46, 1/3, 128, (1993).
[11] FIELDS, D.S. & BACKOFEN, W.A.: Proc. Amer. Soc. Test. Mater., 57, 1263, (1957).
[12] Andrade, H.L.; Akben, M.G. and Jonas, J.J., Metall. Trans. A, 1983, vol. 14A, pp. 1967-1977.
[13] Sun, W. P.; Militzer, M.: Bay, D. Q. and Jonas, J. J.: Acta Metall. Mater., 1993, vol. 41, pp. 3595-3604.